Computers and Geosciences 109 (2017) 323–330

Contents lists available at ScienceDirect

Computers and Geosciences

journal homepage: www.elsevier.com/locate/cageo

Rectification of Image Velocity Results (RIVeR): A simple and user-friendly toolbox for large scale water surface Particle Image Velocimetry (PIV) and Particle Tracking Velocimetry (PTV)

Antoine Patalano *, Carlos Marcelo García, Andrés Rodríguez

Institute for Advanced Studies for Engineering and Technology (IDIT CONICET/UNC), CETA – FCEFyN, Av. Velez Sarsfield 1611, Ciudad Universitaria, Córdoba, Argentina

ARTICLE INFO

Keywords:
LSPIV
LSPTV
Surface-flow measurement
Stream gauging
Velocity mapping

ABSTRACT

LSPIV (Large Scale Particle Image Velocimetry) and LSPTV (Large Scale Particle Tracking Velocimetry) are used as relatively low-cost and non-intrusive techniques for water-surface velocity analysis and flow discharge measurements in rivers or large-scale hydraulic models. This paper describes a methodology based on state-of-the-art tools (for example, that apply classical PIV/PTV analysis) resulting in large-scale surface-flow characterization according to the first operational version of the RIVeR (Rectification of Image Velocity Results). RIVeR is developed in Matlab and is designed to be user-friendly. RIVeR processes large-scale water-surface characterization such as velocity fields or individual trajectories of floating tracers. This work describes the wide range of application of the techniques for comparing measured surface flows in hydraulic physical models to flow discharge estimates for a wide range of flow events in rivers (for example, low and high flows).

1. Introduction

Particle Image Velocimetry (PIV) has been widely used in hydraulics for more than 30 years in laboratory experiments (Adrian, 2005, 1991, 1984). Since the 1980s, various researchers have attempted to adapt PIV techniques to characterize at scales larger than laboratory settings that include the collection of field measurements, the Large Scale Particle Image Velocimetry (LSPIV) (Creutin et al., 2003; Fujita et al., 1998; Gunawan et al., 2012; Le Coz et al., 2014; Muste et al., 2008). LSPIV has been used for water-surface velocity analysis and discharge estimation in rivers. The main difference between PIV (small scale) and LSPIV (large scale) are the flow scales of interest. PIV and LSPIV also differ in the complexities associated to large-scale field measurements, such as variable illumination, and the limited accessibility to orthogonal camera views. Orthogonal camera views require an accurate geometric rectification of the images, or velocity results, to overcome the appreciable distortions produced by the viewing angle of the camera. Similar to PIV, Particle Tracking Velocimetry (PTV) also is a non-intrusive, image-based technique, but PTV is used to determine the velocity associated with individual tracer particles along their trajectories (Baek and Lee, 1996; Brevis et al., 2011; Lloyd et al., 1995; Perkins and Hunt, 1989). This technique is applied in a Lagrangian frame of reference, an important difference with the standard PIV approach, which is applied in an Eulerian frame for example, determining the velocity of groups of tracer particles at fixed spatial positions.

Various free computational tools have been developed during the last 5–10 years for either PIV analysis (for example, OpenPIV, Taylor et al., 2010 or PIVlab, Thielicke and Stamhuis, 2014) or PTV analysis (for example, OpenPTV, Liberzon and Meller, 2013 or PTVlab, Patalano et al., 2013). Their user-friendly Graphical User Interfaces (GUI) contributed to make the non-contact 2-dimensional and 3-dimensional velocity analysis easy to use for laboratory fluid experiments.

Building on the tools and techniques described above, a new, simple toolbox has been developed to complement these tools and techniques to large scale surface flow characterization. To the best of the authors' knowledge, few techniques have been developed for application of LSPIV analysis for hydraulic purposes (Bechle and Wu, 2014; Detert and Weitbrecht, 2015; and Yu et al., 2015). Currently (2016), only one technique is publicly available (Le Coz et al., 2014), and no alternative software is available for LSPTV. The goal of this work is to: a) describe the

Abbreviations: LSPIV, Large Scale Particle Image Velocimetry; LSPTV, Large Scale Particle Tracking Velocimetry; RIVeR, Rectification of Image Velocity Results.

* Corresponding author.
E-mail addresses: antoine.patalano@unc.edu.ar (A. Patalano), carlos.marcelo.garcia@unc.edu.ar (C.M. García), andres.rodriguez@unc.edu.ar (A. Rodríguez).

http://dx.doi.org/10.1016/j.cageo.2017.07.009
Received 28 June 2017; Accepted 29 July 2017

large scale surface-flow characterization system (named Large Scale Analysis system), where the Rectification of Image Velocity Results (RIVeR) toolbox is used; b) describe the first available operational version of the RIVeR toolbox; and c) discuss various applications of the techniques and toolbox.

2. System description

RIVeR is a standalone application developed in the Center for Water Research and Technology (CETA) at the National University of Córdoba, Argentina, beginning in 2013. This application is free of charge and built in Matlab®. A compiled version of the application is currently available at http://riverdischarge.blogspot.com/. RIVeR has been developed in order to provide an efficient experimental large scale water surface characterization (for example, flow velocities and trajectories) and flow discharge estimation in rivers, artificial channels (for example, irrigation, treatment plant, and others.) or large scale hydraulic physical models. Currently (2017), classical PIV/PTV software are constantly being updated and improved with new algorithms, but this software is not adapted for large scale analysis: Therefore, the captured images are oblique and induce deformations and the results need to be rectified. Thus, RIVeR has been developed as an add-on to the available software for producing an efficient large-scale analysis system. A flowchart for the entire large-scale system analysis proposed here is shown in Fig. 1. The modules in blue are parts of the RIVeR toolbox, which is developed in Windows 7 and 10 using Matlab® (release 2015a); the modules in black represent image processing in both PIVlab and PTVlab. The large-scale system analysis introduced here is designed to be user-friendly, low-cost, and flexible. To meet these requirements, the following development strategy is applied:

- Detach video acquisition, image processing, and the rectification tasks so the system can be camera and image processing independent.
- Use of free and updated computational tools.
- Develop a simple and user-friendly interface that allows the system to be used by scientists without advanced computer training.

The large-scale analysis system presented here is composed of three or four major modules, depending on the desired result: Image Extraction, Image Processing, Results Rectification, and Discharge Calculation (optional).

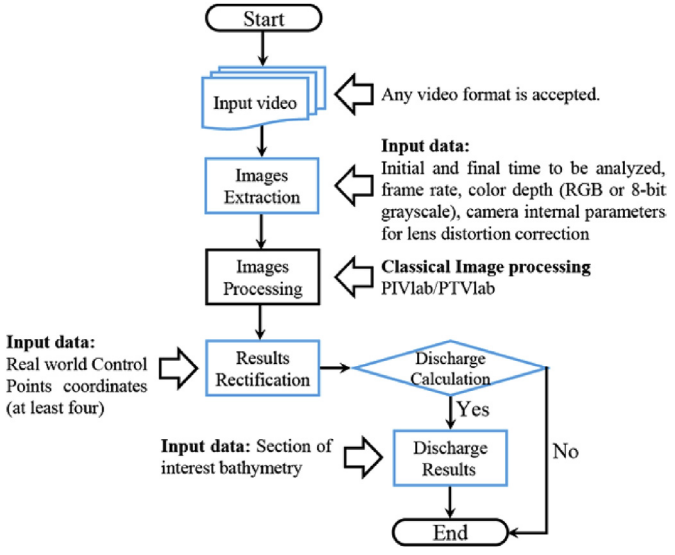

Fig. 1. Flowchart of Large Scale analysis System. Modules in blue are part of the RIVeR toolbox.(For interpretation of the references to colour in this figure legend, the reader is referred to the web version of this article.)

2.1. Images extraction module

The 8-bit grayscale images are extracted from a video through the RIVeR's user interface (Fig. 2) with the free multimedia framework package, ffmpeg (FFmpeg, 2015). The module contains libraries and its developers claim that it "supports the most obscure, ancient video formats right up to the cutting edge" (FFmpeg, 2015). At this step, the frame rate can be resampled, if necessary, considering that the sampling frequency is too high for the flow velocity range that will be analyzed further. An optional lens correction can also be applied if the camera used for the video recording has been previously calibrated by getting the internal parameter settings. The distortion model (Heikkilä and Silvén, 1997) is a Matlab® based subroutine that also is presented in the work done by Taborda and Silva (2012). The subroutine can be described as the following:

$$\begin{pmatrix} X_p \\ Y_p \\ 1 \end{pmatrix} = KK \begin{pmatrix} X_d \\ Y_d \\ 1 \end{pmatrix}, \quad \text{where } KK = \begin{pmatrix} fcx & alpha0{*}fcx & ccx \\ 0 & fcy & ccy \\ 0 & 0 & 1 \end{pmatrix},$$

where X_p, Y_p and X_d, Y_d represent the coordinates of a point in the distorted and undistorted coordinate system, respectively, *fcx* and *fcy* are the focal length in x and y directions, respectively, *cxx* and *ccy* are the image center, and *alpha*0 is the skew coefficient defining the angle between the x and y pixel axes. *KK* is obtained from multiple views of a chessboard of known dimensions with the Camera Calibration Toolbox (Vision Caltech, 2009).

2.2. Images processing module

As described above, the step described here is part of the entire large-scale analysis system but it is performed outside of the RIVeR toolbox. The sub-sequences are shown in Fig. 3 and are described as follows. Please note that the purpose of this paper is not to describe the different algorithms used outside of the RIVeR toolbox, but to describe a new processing technique. The previously extracted images are processed by using either PIVlab or PTVlab with advanced state-of-the-art algorithms, including pre-processing and image enhancement. Using either PIV or PTV analysis for the image series will depend on the desired information and the number and type of tracers used at the water surface. If determining the mean velocity field is the primary purpose of the analysis, (for example, for flow discharge estimation), and the tracers (for example, natural tracers such as foam, tree

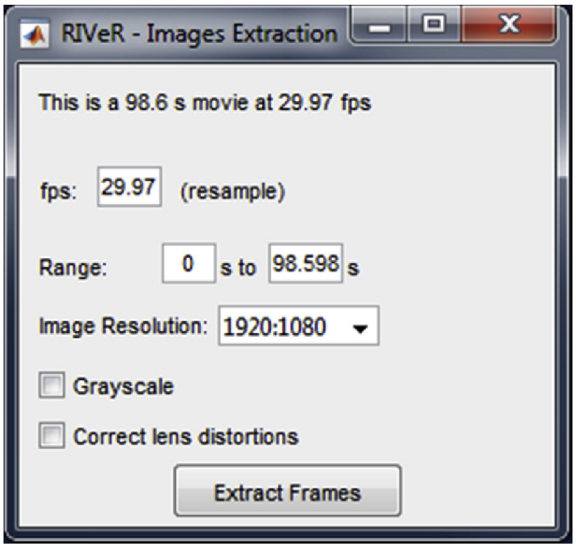

Fig. 2. RIVeR's user interface sample for images extraction.

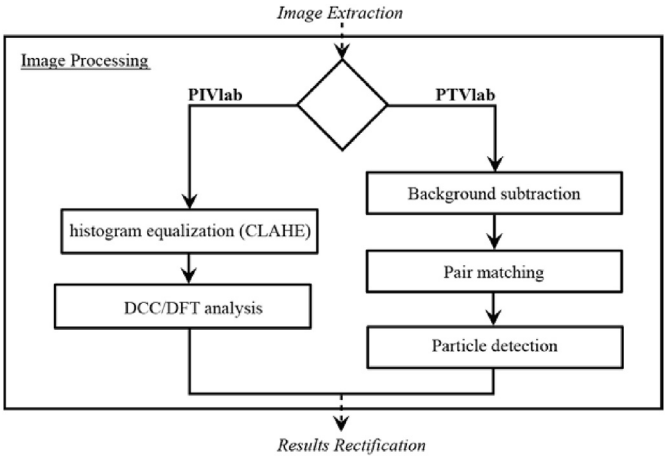

Fig. 3. Flowchart of classical Image Processing sub-sequences with either PIVlab or PTVlab.

branches, and coherent structures at the water surface; artificial tracers such as wood chips or other ecologically harmless and biodegradable material) is homogeneously and densely distributed over the water surface. Afterwards, the images should be analyzed in an Eulerian framework with PIV. Otherwise, if the tracer density is sparse and individual trajectories are required, for example, for flow velocity field characterization near hydraulic structures then PTV should be used in a Lagrangian framework of analysis. For the PIV analysis, PIVlab has been used, which integrates some filters that improve the image processing such as Contrast Limited Adaptive Histogram Equalization (CLAHE). This filter spreads out intensity histograms to the full data range (from 0 to 255 in 8-bit images) and operates in small areas of the image (Pizer et al., 1987). This filter is applied to improve the probability of detecting valid vectors in experimental images. The pixel displacement can be calculated with either the robust Direct Correlation Correlation (DCC) algorithm (Stamhuis, 2006) or the extremely efficient Discrete Fourier Transform (DFT), which calculates the correlation matrix in the frequency domain using FFT (Raffel et al., 2007). The DFT algorithm is multi-pass and uses deformed windows from a pass to the next pass in order to improve the high spatial resolution in the final vector map. For both pixel displacement algorithms, when the integer number indicating the peak location in the correlation matrix is known, a Gaussian function can be fitted to the intensity distribution in order to obtain the sub-pixel displacement.

PTVlab has been used for PTV analysis. In order to improve the particle centroids detection, a preliminary step can be used to remove the image background. Any part of image without motion will be left black. The desired results of this step is that it minimizes the background noise in the image (Honkanen and Nobach, 2005). The Gaussian mask algorithm is used for particle centroid detection. The algorithm searches for particles in the image that match a defined mask with Cross-Correlation (Takehara et al., 2000). The Pair-matching algorithm embedded in PTVlab uses the particle positions in order to calculate the displacement of each particle from an image to the next image with either the Cross-Correlation (CC) algorithm or the combined CC- Relaxation algorithm described in Brevis et al. (2011). The results from both PIVlab and PTVlab are displacements in pixels and the Matlab® result session must be exported. The resulting calculations consist of matrices or vectors of displacement for each pair of analyzed images.

2.3. Results rectification module

After the classical 2-dimensional image processing, the RIVeR toolbox is used again to rectify and make the results completely large scale. In the current version of the toolbox (v2.1), the supported input are Matlab® results sessions from either PIVlab or PTVlab. The Results Rectification is the main module of the toolbox and represents the biggest development of this work. Basically, this step directly relates the real world coordinate system with its 2-dimensional projection on the images. In the following approach, the water surface of the analyzed area of interest in the previous step is presumed to represent the plane that will be rectified. The plane doesn't have to be horizontal because, in some cases (for example, flooded streams), it may be slopped but surface roughness must be small enough so it can be considered as planar. Thus, RIVeR offers the possibility to account for the slope. The so called camera matrix C includes both the intrinsic parameters of the camera (parameters that depend only on the camera such as the focal length, the camera's zoom and the pixel scale), and the extrinsic parameters (camera position and rotation). This approach establishes a direct and unique relation that projects real world coordinates to the image homogeneous system (Corke, 2011):

$$\begin{pmatrix} \tilde{x} \\ \tilde{y} \\ \tilde{z} \end{pmatrix} = \begin{pmatrix} C_{11} & C_{12} & C_{13} & C_{14} \\ C_{21} & C_{22} & C_{23} & C_{24} \\ C_{31} & C_{32} & C_{33} & C_{34} \end{pmatrix} \begin{pmatrix} X_r \\ Y_r \\ Z_r \\ 1 \end{pmatrix}, \quad (1)$$

where $\tilde{x}$, $\tilde{y}$, and $\tilde{z}$ are the components of the homogeneous image coordinates and X, Y, and Z are the real world Cartesian coordinates. The image coordinates in a Cartesian system are calculated as:

$$x = \frac{\tilde{x}}{\tilde{z}}, \quad y = \frac{\tilde{y}}{\tilde{z}}$$

In the following approach, the water surface of the analyzed area of interest in the previous step is presumed to represent the plane that will be rectified. Therefore, the Z components in equation (1) can be ignored and the Camera Matrix C is reduced to the Homography Matrix H (Corke, 2011) and given as equation (2) below.

$$\begin{pmatrix} X_p \\ Y_p \\ 1 \end{pmatrix} = \begin{pmatrix} H_{11} & H_{12} & H_{13} \\ H_{21} & H_{22} & H_{23} \\ H_{31} & H_{32} & 1 \end{pmatrix} \begin{pmatrix} X_r \\ Y_r \\ 1 \end{pmatrix}. \quad (2)$$

Whereas the vector on the left-hand side of equation (2) represents the real world coordinates, the vector on the right-hand side represents the projection of the image on real world coordinates, and H is the homography matrix. Thus, H is left with eight unknowns that can be solved knowing the (X_r, Y_r) coordinates of only four Control Points (CPs), also referred to as Ground Reference Points that are along the same plane. The plane $z = 0$ will be chosen as the water surface. Thus, in order to rectify the results from the image processing, at least four known CPs must be defined at the water-surface plane. It should be noted that the CPs must not be aligned. In the developed RIVeR toolbox, the homography matrix H is calculated using the open-source computer application Camera Calibration Toolbox for MATLAB®, developed by Vision Caltech (2009). Then, once a PIVlab/PTVlab session (including the results) is imported in RIVeR, the results are orthorectified using equation (2). Whereas the Camera Matrix C allows transforming real world coordinates into pixel (Jodeau et al., 2008), the transformation H can be inverted. This inversion indicates that it is possible to transform coordinates in both directions, which is necessary for results rectification, although this is not the case for the Camera Matrix C. Resolving the Homography matrix H, instead of the full Camera matrix, simplifies making the CP measurements because the measurements can be taken with a simple measuring tape, whereas complex instruments are required for taking measurements in 3-dimensional space. Results from either PIVlab or PTVlab are displacements that can be expressed as

$$\overrightarrow{d_i} = X_{pi}^{e} - X_{pi}^{o},$$

where $\vec{d_i}$ is the displacement vector, *and* X^o_{pi} and X^e_{pi} are projected coordinates of the origin and the end of the vector, respectively. Both coordinates are rectified into real world coordinates with equation (2).

The real world displacement is then calculated as

$$\vec{D_i} = X^e_{ri} - X^o_{ri},$$

where $\vec{D_i}$ is the rectified displacement vector, X^o_{ri} and X^e_{ri} are real world coordinates of the origin, and the end of the vector, respectively, and the real world velocity is calculated as

$$\vec{V_i} = \frac{\vec{D_i}}{\Delta t},$$

where Δt is the time step between extracted images that is chosen in the images extraction module, when the frame rate is chosen. For example, for an extraction frame rate of 15 frames per second (fps), the time step is $\Delta t = 66.67$ ms. In the case of PIV analysis, results are then interpolated on a grid defined by the user as the number of nodes in both directions. The number of nodes in both directions are chosen according the measurement procedure suggested by ISO (ISO, 2007). In the case of PTV analysis, particle centroid locations are rectified for each time step.

For the results rectification, the selected CP may be identifiable rocks, structure edges, tree trunks, sticks, and others. RIVeR makes it possible to import tables from Excel® that list CP coordinates in the real world and their projection in pixels (coordinates might also be geographic but this is not a requirement). One of the special features of RIVeR is the four points lengths input. As previously described, at least four not-aligned CPs in the same plane are required for results rectification. A differential global positioning system (GPS) or a topographic survey station are adequate for the real world coordinate measurement and, especially, if more than four CPs are measured. However, these stations make the implementation of LSPIV/LSPTV more expensive. It will be shown that, in some cases, for example, small rivers or physical models, no more than four CPs are required. For most cases, a measuring tape can be used for taking measurements. Because it is difficult to assign coordinates to the CPs with a measuring tape, the distances between each CP (six distances including the diagonals) are measured. Then, a coordinate system is built using the least square method and taking one of the four CPs as the origin. The user interface used for the CPs definition if only four CPs are located by measuring distances between the CPs (Fig. 4). This procedure makes the system simple and affordable to determine. In the case that a fixed camera is used at a site where the stage is variable then C should be solved instead of H in order to rectify the results at different water stages; at least 10 well spread CPs and their 3D coordinates in the real world will be then necessary (Fujita and Kunita, 2011; Le Boursicaud et al., 2016).

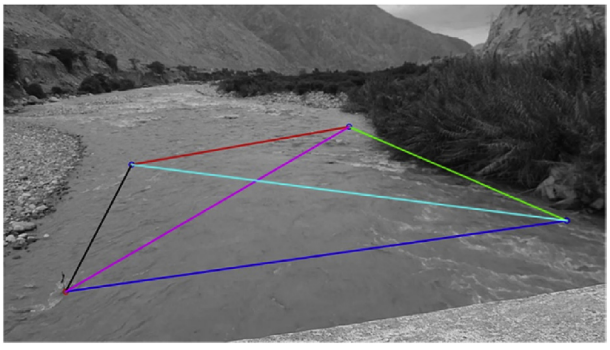

Fig. 4. RIVeR's user interface for Control Points definition (only if the four CP option is used). The distances between each of the four CPs are presented by a different color. The real world distances are required for input to the user interface. View looking upstream.(For interpretation of the references to colour in this figure legend, the reader is referred to the web version of this article.)

Once the homography matrix H is calculated, the velocity vectors are rectified using equation (2) for either PIV or PTV analysis (Fig. 5). A single image may have millions of pixels depending of the camera resolution. The computational time of the entire process is then reduced by rectifying results laying out a grid instead of each pixel position (A 1920×1080 pixels image contains more than 2 million of pixels while a results grids will be limited to a few thousand of vectors). Moreover, the other necessary software can still be developed independently of RIVeR. A single image is also rectified and is used as a background for the results to be overlaid. If the input is a PTVlab session, then the individual particle trajectories are also rectified and plotted with their velocity magnitude (Fig. 5). Rectifying the results instead of the images indicates that RIVeR does not require an appreciable amount of computational time. Most of the computational time needed for the entire process results during the classical PIV and PTV analysis.

2.4. Discharge calculation module

The Discharge Calculation module has been developed for the estimation of flow discharges in different river or channel cross-sections using the mean surface-velocity field computed in the previous module. The streamwise velocity profile extracted from the mean velocity field is shown in Fig. 6. Profile data must cover the entire area of interest. In the case of missing data points, discharge data will be linearly interpolated. If no velocity data are available on transect node, the data will be considered as null, and the rest of the velocity profile will be linearly extrapolated. Once the cross sections are selected, the bathymetry of each section must be imported from an Excel® file for the discharge computations. Moreover, transect geometry is interpolated on the velocity profile grid. In addition, the river stage (water-surface elevation) must be included as an additional input (Fig. 7). As the horizontal distribution of velocity is homogeneously distributed and in practice the measurements might be far away from the banks, the mean section method is applied to compute the total discharge. (ISO, 2007). The method consists in dividing the cross-section in N adjacent verticals at an equal distance d. Thus, Q_s is computed as the sum of the products of the mean depths of two adjacent verticals (h_i and h_{i+1} ,respectively) by the mean of the normal to transect surface-velocity components over those two verticals (V_{si} and V_{si+1} , respectively).

$$Q_s = \sum_{i=1}^{N-1} d \cdot \left(h_i + \frac{h_{i+1}}{2}\right) \cdot \left(V_{s_i} + \frac{V_{s_{i+1}}}{2}\right).$$

The discharge computed Q_s is not exactly the real discharge Q because it has been calculated using the surface-velocity field. Assuming that the vertical velocity profile follows the log-law (Te Chow, 1959), the theoretical ratio between the mean flow velocity and the surface velocity is $\alpha = 0.85$. This value is generally used for uniform flow of average roughness (for example, Le Coz et al., 2010). Thus, the real discharge must be calculated as follow:

$$Q = \alpha \cdot Q_s.$$

The ratio α depends on many parameters, such as the geometry section, the bed roughness, the geometry upstream and downstream the section, secondary flows, and others. It is up to the user to choose the most reliable value of α. Cheng et al. (2004) concluded that it is reliable to use the surface velocity as an index to determine a river flow discharge because the value of α always falls in the same range from 0.80 to 0.93.

3. Applications

LSPIV/LSPTV can be applied as an alternative technique for surface-

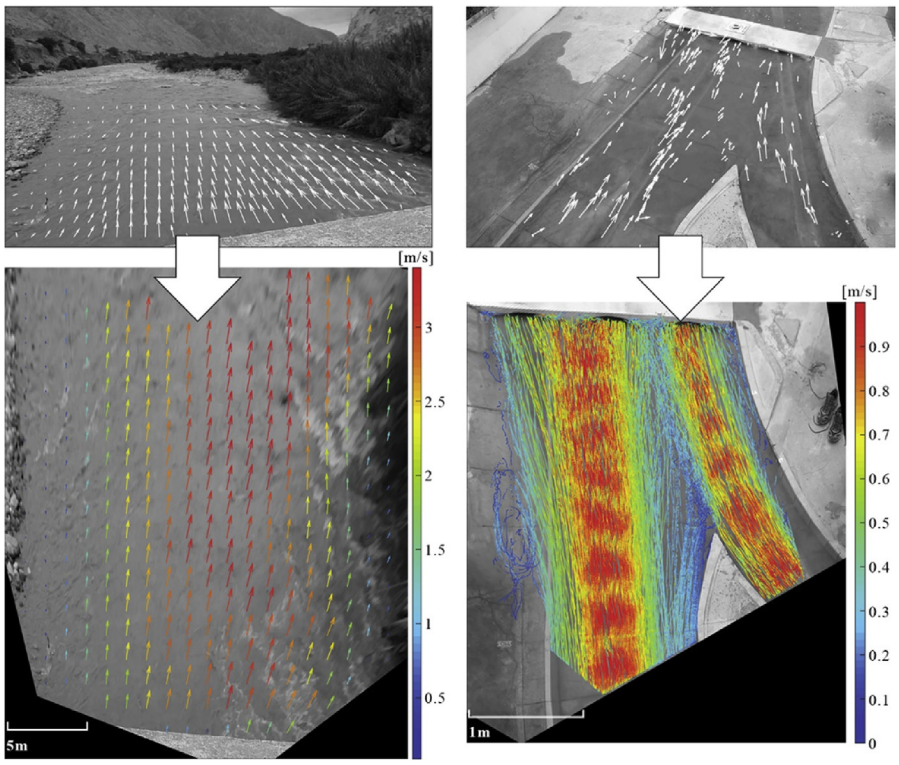

Fig. 5. Rectification results from LSPIV and LSPTV analysis using RIVeR. On the left-hand side: LSPIV, images were recorded in the Pisco River in Perú. From the top to the bottom: Image processing with PIVlab; rectifying velocity field. On the right-hand side: LSPTV, images were recorded in a large-scale physical model in Argentina. From the top to the bottom: Image processing with PTVlab; rectifying individual trajectories.

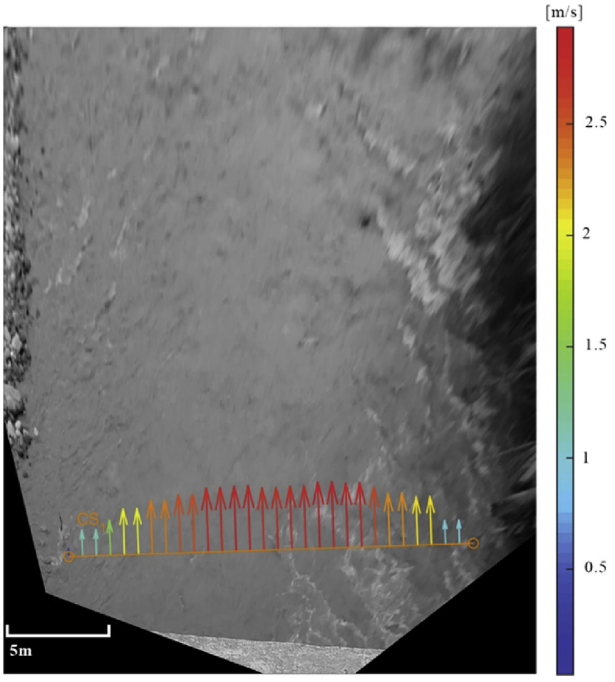

Fig. 6. Mean streamwise surface velocity profile for a selected cross-section. The velocity profile is overlaid on a single rectified background image.

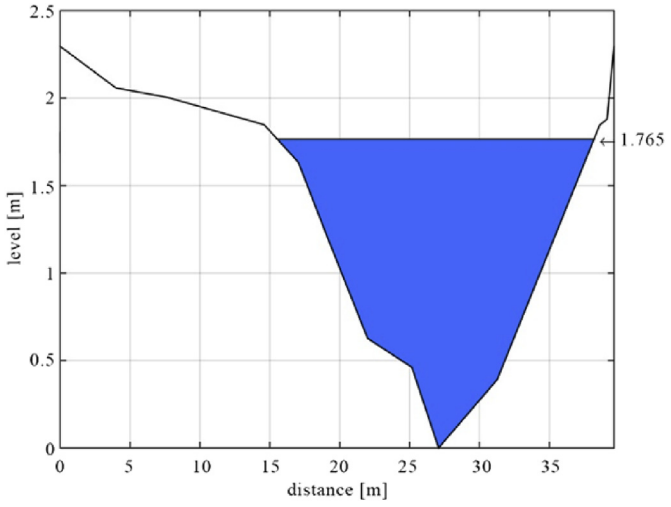

Fig. 7. Cross-section (see Fig. 6) bathymetry imported with the available water stage.

flow characterization in flow conditions where none of the available velocimetry techniques can be used. For example, LSPIV/LSPTV is extremely well-suited for discharge estimation of low (shallow water) (Patalano et al., 2014) and high flows (for example, a flash flood) (Le Coz et al., 2010; Patalano et al., 2015). In both flow regimes, the use of an Acoustic Doppler Current Profiler (ADCP), recognized as the most applied velocimetry technique in river and channels, is difficult or impossible to apply because of the lowflow depths (shallow water) and the unsteady flows [high flow (flash flood)]. Additionally, LSPIV was used here for flow characterization in highly turbulent flows with air incorporated and high velocities (up to 15 m/s in dam spillways; see Fig. 8). This application precludes the use of any other available technique.

RIVeR is used here for flow discharge estimation made from amateur videos recorded during flash-flood events (Fig. 9). This work involves an additional step that includes the video shake removal,

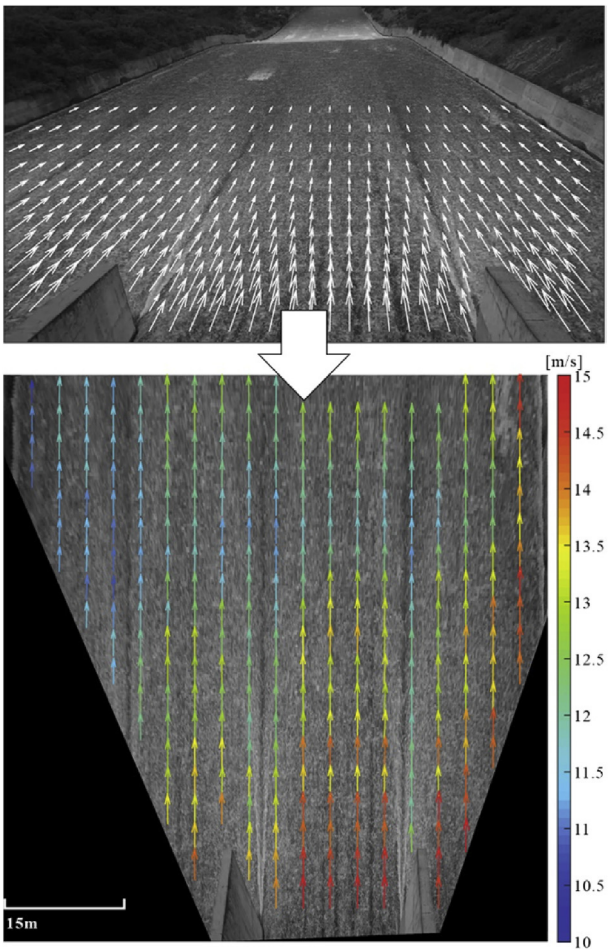

Fig. 8. LSPIV Application in a dam spillway, "Arroyo Corto" Dam, Córdoba, Argentina. On the top: original extracted image, on the bottom: rectified flow velocity field obtained with RIVeR.

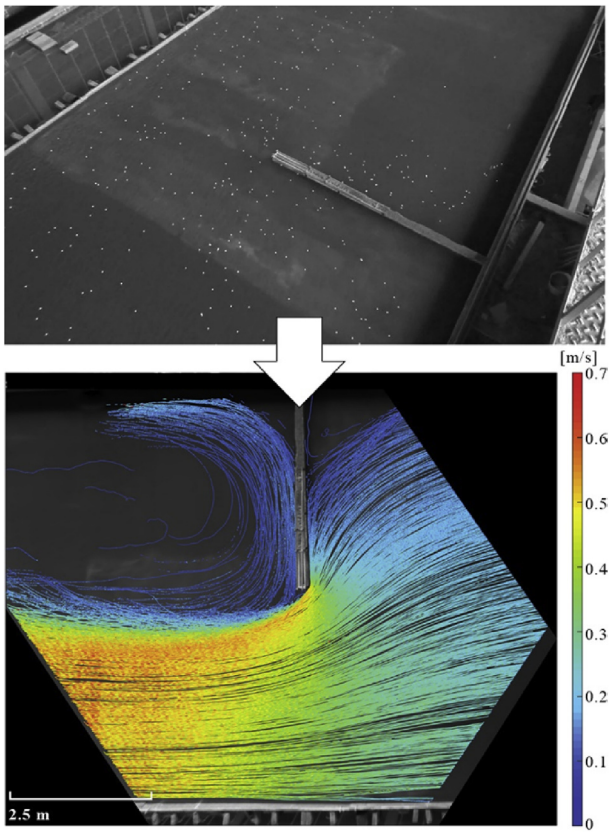

Fig. 10. LSPTV Application in a large scale physical model of a bridge abutment at the National University of the Litoral, Santa Fe, Argentina. Flow was seeded with white 15 mm diameter polystyrene balls (white dots on photograph) to enhance flow visibility.

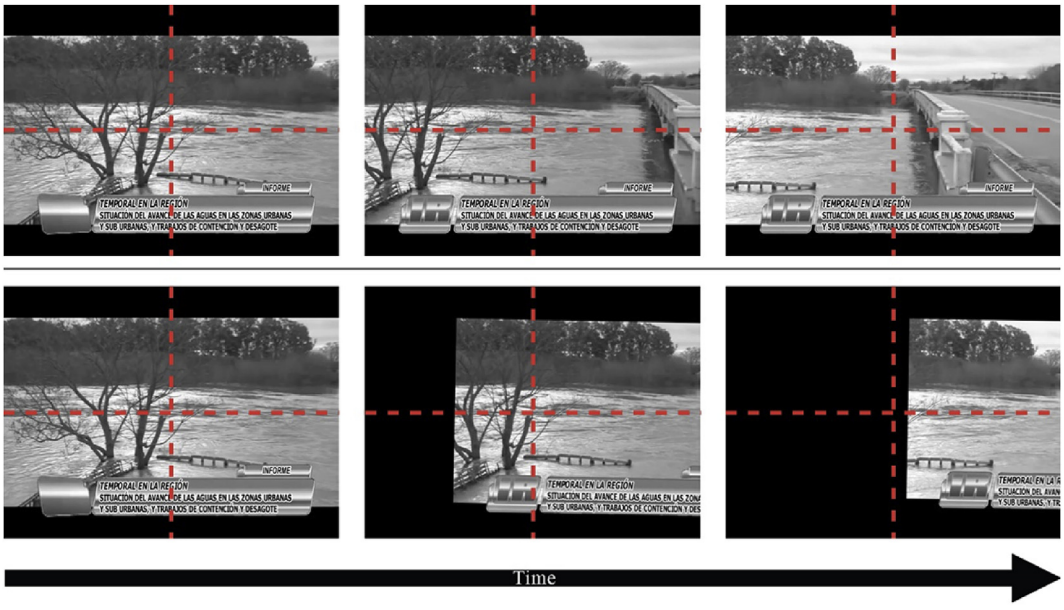

Fig. 9. Original extracted images from an amateur video. The red target has been added and is fixed in order to show the camera panning movement from left to right. Sante Fe, Argentina.(For interpretation of the references to colour in this figure legend, the reader is referred to the web version of this article.)

originally developed by the authors for LSPIV from an Unmanned Aerial Vehicle.

LSPTV can be also used for flow discharge measurement, but the Lagrangian information is a major advantage for flow characterization near hydraulic structures or hydraulic physical model (Fig. 10). Moreover, the velocity measured is the real velocity and no velocity is measured where no water particle is present avoiding low bias in the case of low density particles.

4. Conclusions

This work describes RIVeR, a practical and user-friendly toolbox for large scale PIV and PTV techniques. The freeware should be seen as an add-on to the available image-velocity processing toolboxes such as PIVlab or PTVlab. RIVeR rectifies results from image-velocity processing by solving the homography matrix H that is the reduced form of the camera matrix assuming that all CPs and the free surface are assumed to be in the same plane. Currently (2016), RIVeR is operational and already has been successfully applied in South America. Also, the U.S. Geological Survey (USGS) has been testing the techniques in Illinois since December 2015. The LSPIV and LSPTV techniques are used for flow discharge measurement during high-flow events (for example, flashfloods) and low-flow events. The freeware is also a useful tool for synoptic water-surface characterization of large-scale physical models in laboratories and flow over hydraulic structures. Hydrologists and civil and environmental engineers, and technicians are encouraged to apply these techniques. A quick start guide is included in the last release of the freeware and a forum is available at http://riverdischarge.blogspot.com/. Source code can be downloaded from a GitHub respositoryt at https://github.com/APatal/RIVeR. With the next release, the full Camera matrix will be solved by using various CPs in 3-dimensional space. Also, a generic format will be allowed as input so results from other image-velocity software can be used; for example, optical flow (Dérian et al., 2013; Liu et al., 2003) or STIV (Fujita et al., 2007). Improving the Discharge Computation module is also one of the main target implementing the entropy method explained in Chen and Chiu (2004), Chiu and Said (1995) and also applied in Bechle and Wu (2014) to estimate the ratio between surface and mean depth flow velocities. The authors also are currently working on a smart system based on RIVeR for remote and real time discharge computation with fixed cameras as gaging stations where the Camera matrix will be dynamically calculated for the different water stages.

Acknowledgment

A heartfelt thank you to the researchers from the National University of the Litoral, Santa- Fe, Argentina for providing the experimental facilities where LSPTV was implemented. The authors acknowledge Angel M. Martin, Jr., USGS retired, for his technical edit and constructive comments on the manuscript; Kevin A. Oberg, USGS - Office of Surface Water, for helping in the final edition of this work; and two anonymous reviewers provided useful comments and suggestions for improving the manuscript.

References

Adrian, R.J., 1984. Scattering particle characteristics and their effect on pulsed laser measurements of fluid flow: speckle velocimetry vs particle image velocimetry. Appl. Opt. 10–11.

Adrian, R.J., 1991. Particle-imaging techniques for experimental fluid-mechanics. Annu. Rev. Fluid Mech. 23, 261–304. http://dx.doi.org/10.1146/annurev.fluid.23.1.261.

Adrian, R.J., 2005. Twenty years of particle image velocimetry. Exp. Fluids 39, 159–169. http://dx.doi.org/10.1007/s00348-005-0991-7.

Baek, S.J., Lee, S.J., 1996. A new two-frame particle tracking algorithm using match probability. Exp. Fluids 22, 23–32. http://dx.doi.org/10.1007/BF01893303.

Bechle, A.J., Wu, C.H., 2014. An entropy-based surface velocity method for estuarine discharge measurement. Water Resour. Res. 50, 6106–6128. http://dx.doi.org/10.1002/2014WR015353.

Brevis, W., Niño, Y., Jirka, G.H., 2011. Integrating cross-correlation and relaxation algorithms for particle tracking velocimetry. Exp. Fluids 135–147. http://dx.doi.org/10.1007/s00348-010-0907-z.

Chen, Y.-C., Chiu, C.-L., 2004. A fast method of flood discharge estimation. Hydrol. Process 18, 1671–1684. http://dx.doi.org/10.1002/hyp.1476.

Cheng, R.T., Gartner, J.W., Mason, R.R., Costa, J.E., Plant, W.J., Spicer, K.R., Haeni, F.P., Melcher, N.B., Keller, W.C., Hayes, K., 2004. Evaluating a Radar-based, Non Contact Streamflow Measurement System in the San Joaquin River at Vernalis, California. Menlo Park, California.

Chiu, C.-L., Said, C.A.A., 1995. Maximum and mean velocities and entropy in open-channel flow. J. Hydraul. Eng. 121, 26–35. http://dx.doi.org/10.1061/(ASCE)0733-9429(1995)121:1(26).

Corke, P., 2011. Robotics, Vision and Control, Springer Tracts in Advanced Robotics. Springer Berlin Heidelberg, Berlin, Heidelberg. http://dx.doi.org/10.1007/978-3-642-20144-8.

Creutin, J.-D., Muste, M., Bradley, A., Kim, S.C., Kruger, A., 2003. River gauging using PIV techniques: a proof of concept experiment on the Iowa River. J. Hydrol. 277, 182–194. http://dx.doi.org/10.1016/S0022-1694(03)00081-7.

Dérian, P., Héas, P., Herzet, C., Mémin, É., 2013. Wavelets and optical flow motion estimation. Numer. Math. Theory Methods Appl. 116–137. Glob. Sci. Press.

Detert, M., Weitbrecht, V., 2015. A low-cost airborne velocimetry system: proof of concept. J. Hydraul. Res. 53, 532–539. http://dx.doi.org/10.1080/00221686.2015.1054322.

FFmpeg, 2015. https://www.ffmpeg.org/.

Fujita, I., Kunita, Y., 2011. Application of aerial LSPIV to the 2002 flood of the Yodo River using a helicopter mounted high density video camera. J. Hydro-environ. Res. 5, 323–331. http://dx.doi.org/10.1016/j.jher.2011.05.003.

Fujita, I., Muste, M., Kruger, A., 1998. Large-scale Particle Image Velocimetry for flow analysis in hydraulic engineering applications. J. Hydraul. Res. 36, 397–414. http://dx.doi.org/10.1080/00221689809498626.

Fujita, I., Watanabe, H., Tsubaki, R., 2007. Development of a non-intrusive and efficient flow monitoring technique: the space-time image velocimetry (STIV). Int. J. River Basin Manag. 5, 105–114. http://dx.doi.org/10.1080/15715124.2007.9635310.

Gunawan, B., Sun, X., Sterling, M., Shiono, K., Tsubaki, R., Rameshwaran, P., Knight, D.W., Chandler, J.H., Tang, X., Fujita, I., 2012. The application of LS-PIV to a small irregular river for inbank and overbank flows. Flow. Meas. Instrum. 24, 1–12. http://dx.doi.org/10.1016/j.flowmeasinst.2012.02.001.

Heikkilä, J., Silvén, O., 1997. A four-step camera calibration procedure with implicit image correction. In: IEEE Computer Society Conference on Computer Vision and Pattern Recognition (CVPR'97). San Ruan, Puerto Rico, pp. 1106–1112.

Honkanen, M., Nobach, H., 2005. Background extraction from double-frame PIV images. Exp. Fluids 38, 348–362. http://dx.doi.org/10.1007/s00348-004-0916-x.

ISO, 2007. Hydrometry - Measurement of Liquid Flow in Open Channels Using Current - Meters or Floats. ISO 748:2007(E).

Jodeau, M., Hauet, A., Paquier, A., Le Coz, J., Dramais, G., 2008. Application and evaluation of LS-PIV technique for the monitoring of river surface velocities in high flow conditions. Flow. Meas. Instrum. 19, 117–127. http://dx.doi.org/10.1016/j.flowmeasinst.2007.11.004.

Le Boursicaud, R., Pénard, L., Hauet, A., Thollet, F., Le Coz, J., 2016. Gauging extreme floods on YouTube: application of LSPIV to home movies for the post-event determination of stream discharges. Hydrol. Process 30, 90–105. http://dx.doi.org/10.1002/hyp.10532.

Le Coz, J., Hauet, A., Pierrefeu, G., Dramais, G., Camenen, B., 2010. Performance of image-based velocimetry (LSPIV) applied to flash-flood discharge measurements in Mediterranean rivers. J. Hydrol. 394, 42–52. http://dx.doi.org/10.1016/j.jhydrol.2010.05.049.

Le Coz, J., Jodeau, M., Hauet, A., Marchand, B., Le Boursicaud, R., 2014. Image-based velocity and discharge measurements in field and laboratory river engineering studies using the free F UDAA -LSPIV software. In: River Flow. Lausanne, Switzerland.

Liberzon, A., Meller, Y., 2013. Openptv. https://github.com/OpenPTV.

Liu, H., Chellappa, R., Rosenfeld, A., 2003. Fast two-frame multiscale dense optical flow estimation using discrete wavelet filters. J. Opt. Soc. Am. A. Opt. Image Sci. Vis. 20, 1505–1515.

Lloyd, P.M., Stansby, P.K., Ball, D.J., 1995. Unsteady surface-velocity field measurement using particle tracking velocimetry. J. Hydraul. Res. 33, 519–534. http://dx.doi.org/10.1080/00221689509498658.

Muste, M., Fujita, I., Hauet, A., 2008. Large-scale Particle Image Velocimetry for measurements in riverine environments. Water Resour. Res. 44, 1–14. http://dx.doi.org/10.1029/2008WR006950.

Patalano, A., Brevis, W., García, C.M., Bleninger, T., Rodríguez, A., 2013. PTVlab, una herramienta grafica para el procesamiento digital en Velocimetría por Seguimiento de Partículas. In: Tercer Simposio de Metodos Experimentales En Hidraulica. Santa Fe, Argentina.

Patalano, A., García, C.M., Guillén, N., García, C., Díaz, É., Rodriguez, A., Ravelo, A., 2014. Evaluación experimental de la técnica de velocimetría por seguimiento de partículas a gran escala para la determinación de caudales en Ríos serranos. Aqua-LAC UNESCO 6, 17–24.

Patalano, A., García, C.M., Guillén, N.F., Catalini, C., García, C.L., Ravelo, A., 2015. Implementación de la técnica de lspiv para la cuantificación de caudales en Ríos durante crecidas utilizando un vehículo aéreo no tripulado. In: IV Simposio Sobre Métodos Experimentales En Hidráulica. La Plata, Argentina.

Perkins, R.J., Hunt, J.C.R., 1989. Particle tracking in turbulent flows. Adv. Turbul. 2, 286–291.

Pizer, S.M., Amburn, E.P., Austin, J.D., Cromartie, R., Geselowitz, A., Greer, T., Ter Haar Romeny, B., Zimmerman, J.B., Zuiderveld, K., 1987. Adaptive histogram equalization and its variations. Comput. Vis. Graph. Image Process 39, 355–368. http://dx.doi.org/10.1016/S0734-189X(87)80186-X.

Raffel, M., Willert Christian, E., Wereley, S.T., Kompenhans, J., 2007. Particle Image Velocimetry, Experimental Fluid Mechanics. Springer Berlin Heidelberg, Berlin, Heidelberg. http://dx.doi.org/10.1007/978-3-540-72308-0.

Stamhuis, E.J., 2006. Basics and principles of Particle Image Velocimetry (PIV) for mapping biogenic and biologically relevant flows. Aquat. Ecol. 40, 463–479. http://dx.doi.org/10.1007/s10452-005-6567-z.

Taborda, R., Silva, A., 2012. COSMOS: a lightweight coastal video monitoring system. Comput. Geosci. http://dx.doi.org/10.1016/j.cageo.2012.07.013.

Takehara, K., Adrian, R.J., Etoh, G.T., Christensen, K.T., 2000. A Kalman tracker for super-resolution PIV. Exp. Fluids 29, S034–S041. http://dx.doi.org/10.1007/s003480070005.

Taylor, Z.J., Gurka, R., Kopp, G.A., Liberzon, A., 2010. Long-duration time-resolved PIV to study unsteady aerodynamics. IEEE Trans. Instrum. Meas. 59, 3262–3269. http://dx.doi.org/10.1109/TIM.2010.2047149.

Te Chow, V., 1959. Open-channel Hydraulics. McGraw-Hill Higher Education, Tokyo.

Thielicke, W., Stamhuis, E.J., 2014. PIVlab – towards user-friendly, affordable and accurate digital Particle Image Velocimetry in MATLAB. J. Open Res. Softw. 2 http://dx.doi.org/10.5334/jors.bl.

Vision Caltech, 2009. Camera Calibration Toolbox for Matlab. http://www.vision.caltech.edu/bouguetj/calib_doc/.

Yu, K., Kim, S., Kim, D., 2015. Correlation analysis of spatio-temporal images for estimating two-dimensional flow velocity field in a rotating flow condition. J. Hydrol. 529, 1810–1822. http://dx.doi.org/10.1016/j.jhydrol.2015.08.005.